Applied Biochemistry and Biotechnology (2019) 188:952–964
https://doi.org/10.1007/s12010-019-02967-6

Preparation of an Electrically Conductive Graphene Oxide/Chitosan Scaffold for Cardiac Tissue Engineering

Lili Jiang[1] · Daoyu Chen[1] · Zhen Wang[1] · Zhongmin Zhang[1] · Yangliu Xia[1] · Hongyu Xue[1] · Yong Liu[1]

Received: 8 November 2018 / Accepted: 30 January 2019 /
Published online: 11 February 2019
© Springer Science+Business Media, LLC, part of Springer Nature 2019

Abstract

Cardiac tissue engineering is of great importance for therapeutic and pharmaceutical applications. The scaffolds that can provide electrical conductivity and structural organization will be highly beneficial for cardiac tissue engineering. Here, we developed conductive scaffolds with electrical conductivity and porous structure composed of chitosan (CS) blending with graphene oxide (GO) for cardiac tissue engineering. Our results showed that the swelling, porosity, and conductive properties of GO/CS scaffolds could be modulated via adjusting the ratio of GO to CS. More importantly, GO/CS scaffolds had a swelling ratio ranging from 23.20 to 27.38 (1000%) and their conductivity (0.134 S/m) fell in the range of reported conductivities for native cardiac tissue. Furthermore, we assessed their biological activity by seeding heart H9C2 cells in GO/CS scaffolds. Our data showed that these GO/CS scaffolds exhibited good cell viability, promotion of cell attachment and intercellular network formation, and upregulation of the cardiac-specific gene and protein expression involved in muscle conduction of electrical signals (Connexin-43). Overall, it is concluded that the GO/CS scaffolds promote the properties of cardiac tissue constructs. Our findings provide a new strategy and insight in developing new scaffolds for cardiac tissue engineering.

Keywords Cardiac tissue engineering · Cardiomyocytes · Conductive scaffolds · Chitosan · Graphene oxide

Introduction

Myocardial infarction (MI), commonly known as a heart attack, is associated with significant cell death and consequently leads to loss of heart function [1]. When MI occurs, due to a

Electronic supplementary material The online version of this article (https://doi.org/10.1007/s12010-019-02967-6) contains supplementary material, which is available to authorized users.

✉ Yong Liu
yliu@dlut.edu.cn

[1] School of Life Science and Medicine, Dalian University of Technology, 2 Dagong Road, Liaodongwan New District, Panjin 124221, China

minimal regeneration potential of cardiomyocytes, the damaged adult heart muscle has a poor capability to repair itself [2]. So far, heart transplantation, cell therapy, and tissue engineering have been considered as promising strategies for the treatment of MI. Among them, cardiac tissue engineering offers a promising approach to repair damaged heart tissue thanks to the engineering of three-dimensional (3D) cellularized tissue constructs provided by 3D proper scaffolds [3].

In the past few years, various synthetic and natural materials have been proposed as scaffolds to be used for cardiac tissue engineering applications [2, 4–6]. Chitosan (CS), an abundant natural product, is an ideal material for tissue engineering due to its outstanding biocompatibility, antibacterial, and immunologic activity [7–11]. The CS cardiac scaffolds have been found to promote interconnectivity of cells [12] and improve the cardiac function following MI [13, 14].

Although CS scaffolds can offer extracellular matrix-like microenvironment to support cardiac cell functions, poor electrical properties of these CS scaffolds limit to replicate the characteristics of the native myocardium [15, 16]. Since these CS scaffolds are nonconductive, their electrical properties can be improved by adding conductive material such as graphene oxide (GO). GO is an ideal material as it possesses limited cytotoxicity, enhances mechanical properties, and is responsive for electrical signal conduction [17, 18]. Cardiomyocytes cultured in scaffolds containing GO have demonstrated enhanced adhesion, proliferation, and expression of cardiac-specific markers [19]. GO can therefore greatly improve the performance of cardiac scaffolds by allowing enhanced cell–cell communication and hence supporting the re-establishment of synchronous contractile activity in the scaffolds.

Here, we aimed to generate a novel electrically conductive scaffold based on GO and CS for cardiac tissue engineering. We hypothesized that GO/CS scaffolds would improve cardiomyocytes function by increasing expression of connexin-43 (CX-43) protein even without electrical stimulation. Our strategy was to combine the biocompatibility and biodegradability of CS with the electrical properties of GO. Furthermore, H9C2 cells were seeded into the conductive scaffolds, and their viabilities and expression of the cardiac-specific genes and proteins were studied.

Materials and Methods

Preparation of GO/CS Scaffolds

GO/CS scaffolds were fabricated by freezing and lyophilization of GO solution blended CS powder as reported previously [8]. Briefly, to synthesize composite electronically conductive polyporous scaffolds with different fractions of GO (50, 100, 150, 600 mg/L of GO), the CS power (20 g/L) was ultrasonically dispersed in different concentration GO solutions for 30 min. Then the acetic acid was slowly dropped into suspension in the ratio 0.6% (*v*/*v*). Subsequently, GO/CS dispersions were vigorously mixed using a magnetic stirrer for 12 h at room temperature to obtain a homogenous mixture. Next, the obtained GO/CS dispersions were transferred to 96-well plates, frozen at − 80 °C for 48 h and lyophilized in a freeze dryer (LABCONCO FreeZone Triad Freeze Dry Systems). Pure CS scaffolds were also fabricated as controls. Following immersing with 100% ethanol for 12 h, the GO/CS electrically conductive scaffolds were washed three times with distilled water (30 min each). The pure CS and GO/CS scaffolds were then sterilized under a UV lamp for 30 min.

Physical Characterization of the Scaffolds

Scanning Electron Microscopy Analysis

To study the microstructure morphology, pore features of the scaffolds, and cardiomyocytes adhesion on scaffold, the samples were examined with scanning electron microscopy (Nova NanoSEM 450, Thermo Fisher Scientific) as reported previously [20]. Briefly, the samples were washed with PBS and then were fixed with 2.5% glutaraldehyde for 30 min. After this, the samples were dehydrated with 30%, 50%, 70%, 80%, 90%, 95%, and 100% ethanol for 10 min each. Following incubating in 50% Hexamethyl Disilazane (50% Hexamethyl Disilazane and 50% ethanol) for 10 min, the samples were soaked in 100% Hexamethyl Disilazane for 5 min and dried overnight under vacuum. At last, three dry samples for each group were coated with gold powder using a high-resolution turbomolecular pumped sputter coater (Nicolet iS 50, Thermo Fisher Scientific) for enhanced conductivity, and observed under an operating voltage of 20 kV.

Swelling Behavior Analysis

The swelling ratios of the scaffolds were determined gravimetrically by incubating pre-weighed GO/CS composite scaffolds with different contents of GO in PBS (pH 7.4) at 37 °C [21]. Briefly, lyophilized samples were immersed in PBS (pH 7.4) at 37 °C for 24 h, and the swollen weight of the scaffolds was recorded after removal of excess water using filter paper. The swelling ratios were calculated according to the following equation:

$$\text{Swelling ration } (\%) = ((W_s - W))/W \times 100 \tag{1}$$

where W_s and W represented the swollen and dry weights of the samples, respectively. All experiments were separately performed in triplicate.

Porosity Analysis

The porosity of different concentration GO/CS scaffolds was evaluated by liquid displacement method [22] using ethanol and gravity bottle. The scaffolds (dry weight) were immersed in the ethanol for 2 h, and the weight of the scaffolds in gravity bottle filled with ethanol was considered. The porosity of the scaffolds was measured according to the following equations:

$$\text{Porosity} = (1 - m1/(v \times \rho_{real})) \times 100\% \tag{2}$$

$$\rho_{real} = (m1 \times \rho_{ethanol})/(m1 + m2 - m3) \tag{3}$$

where $m1$ represented dry weights of the scaffolds, $m2$ represented weights of gravity bottle filled with alcohol, and $m3$ represented weights of gravity bottle fitted with alcohol and dry scaffolds. The data were shown as a mean ± SD ($n = 3$).

Electrical Conductivity Analysis

The electrical conductivity of the GO/CS composite scaffolds was measured with electrochemical workstation (PARSTAT MC, Princeton, USA) by using a previously published method [23]. The two thin metal electrodes were used to join two ends of the scaffolds. Electrical conductivity was calculated by measuring the voltage drop across the two electrodes. The experimental determination was repeated three times for each sample to evaluate the sample accuracy. The electrical conductivity (σ) was calculated using the following formula:

$$\sigma = (1/AL) \times (I/V) \tag{4}$$

where A was the area of the electrodes, L was the thickness of the scaffolds, I was the current, V was the voltage, and σ was electrical conductivity.

Biological Characterization of the Scaffolds

Cytotoxicity Analysis

The cytotoxicity of GO/CS scaffolds in vitro was assessed using MTT (Sigma) assay on the seventh day [24]. Briefly, all scaffolds were sterilized by immersing in 75% ethanol for 12 h, rinsing with sterile phosphate buffered saline (PBS) three times, and prewetting with culture medium (DMEM) overnight. Then all scaffolds were seeded with 2×10^6 cells/mL cells suspension (10 μL per scaffold). Optical density (OD) from various ration GO/CS scaffolds and CS scaffold was detected using a microplate system (Synergy H1, BioTek). All measurements were performed in triplicate.

Western Blot

To investigate the influence of scaffolds on cardiac-specific proteins, two of the positive control factors for the conductive function of cardiac tissue, connexin-43 (CX-43) and cardiac troponin T (cTnT), were detected with western blot analysis with the method described previously [25]. Total protein was extracted from the scaffolds seeded with cardiomyocytes (H9C2 cells) after 7 days of cultivation. We performed western blotting with anti-connexin-43 antibody and anti-cardiac troponin T antibody as described [26]. Briefly, samples were denatured in boiling water for 3 min. Then samples were resolved by 12% sodium dodecyl sulfate–polyacrylamide gel electrophoresis. After transferring onto a PVDF membrane (Millipore, USA), the membrane was blocked 5% skimmed milk powder in PBS and then incubated in primary antibodies overnight at 4 °C. The membrane was incubated in secondary antibodies for 1 h at room temperature and was detected using the Enhanced Chemiluminescence (ECL Plus) system. All antibodies for Western blot analysis were purchased from Abcam (USA). Results were reproducible in repeated experiments.

RNA Extraction and Real-time Reverse Transcription PCR

The expression of specific cardiac makers including cardiac troponin T and connexin-43 were analyzed by real-time quantitative PCR [27]. After 7 days of cultivation, scaffolds with cardiomyocytes (H9C2 cells) were harvested for the evaluation of the mRNA levels of specific

cardiac genes. Total RNAs were extracted by using RNeasy kit (Takara, Japan) according to the manufacturer's protocols. The primer pairs used for Real-time PCR reaction were listed in Table 1. Complementary DNA (cDNA) was prepared by utilizing PrimeScript™ RT reagent Kit (Perfect Real Time) (Takara, Japan). Quantitative real-time PCR was performed using the SYBR^{R} *Premix Ex* Taq™ II (Tli RNaseH Plus) (Takara, Japan). All cycle threshold (Ct) values calculated from the target genes were normalized to housekeeping gene such as β-actin, and data were calculated as fold change relative to the control.

Statistical Analysis

Statistical analysis was performed by GraphPad Prism 5 software (GraphPad Software, USA). Results were expressed as mean ± standard deviations, and 95% confidence limits were calculated for each set of results. Data were compared using one-way ANOVA. A p value < 0.05 indicated statistical significance.

Results

Influence of GO Concentration on Scaffold Macro- and Microscopic Structure

To explore the influences of GO concentrations on morphological of GO/CS scaffolds, we observed the macro- and microscopic structure of the GO/CS scaffolds with different concentrations. Table 2 showed representative samples of pure CS scaffold and of GO/CS scaffolds composites containing different concentrations of GO. Figure 1 showed the effects of GO concentration on morphological and structural properties. As shown in Fig. 1, all samples, including CS scaffold and GO/CS scaffolds, exhibited the similar sponge-like microstructure after lyophilization. The color of the samples darkened with increasing concentration of GO in the composites (Fig. 1a). Furthermore, SEM analysis showed that all samples had similar anisotropic and symmetric porous structures irrespective of GO concentration (Fig. 1b). However, scaffolds with GO had smaller pore diameter distributions than that without GO.

Influence of GO Concentration on Scaffold Swelling and Porosity

The ability of a scaffold to absorb and retain water is an important characteristic for assessing its biocompatibility for cardiac tissue engineering. The effects of GO concentration on swelling ratio of scaffolds were shown in Fig. 2a. The swelling ratio of GO/CS scaffolds decreased with

Table 1 Primers used for RT-PCR

Gene	Primer sequence (5′–3′)	Number bases	Annealing (°C)
Connexin-43	TCTTCATGCTGGTGGTGTCC	20	57.7
	AGTGGTGGCGTGGTAAGGAT	20	59.0
cTnT	GACGAGCAAGAGGAGGCAGT	20	60.1
	TGGCTTCTTCATCAGGACCA	20	56.0
β-actin	TGTCACCAACTGGGACGATA	20	58.37
	GGGGTGTTGAAGGTCTCAAA	20	57.46

Table 2 Composition of CS/GO scaffolds

Scaffold	CS solution (0.6% acetic acid)	GO (aqueous solution)	GO/CS
GO/CS 1	20 g/L	0 mg/L	0
GO/CS 2	20 g/L	50 mg/L	50
GO/CS 3	20 g/L	100 mg/L	100
GO/CS 4	20 g/L	150 mg/L	150
GO/CS 5	20 g/L	600 mg/L	600

GO concentration, but there were no significant differences compared with a non-GO scaffold (0 mg/L) except for 600 mg/L GO/CS scaffold ($p < 0.05$).

An important criterion of a scaffold is the interconnected porous structure. The effects of GO concentration on the porosity of scaffolds were assessed and were shown in Fig. 2b. All the scaffolds possessed of the similar porosity (83–90%). The porosity of scaffolds decreased with GO concentration, but there were no significant differences compared with a non-GO scaffold (0 mg/L) unless 600 mg/L GO/CS scaffold ($p < 0.05$).

Influence of GO Concentration on Cell Viability

The influences of GO concentration on cell activities were assessed by MTT assays, and the results were shown in Fig. 2c. After 7 days of cultivation, cell activities decreased with GO concentrations. The percentage of cell activities were over 80% in low concentration (0, 50,100,150 mg/L) GO/CS scaffolds, and there were no significant differences compared with the non-GO scaffold. However, 600 mg/L GO/CS scaffold caused a significant reduction in cell viability (< 60%) ($p < 0.05$). Based on the above the results, the suitable concentration for GO/CS scaffolds was likely to be 150 mg/L taking into

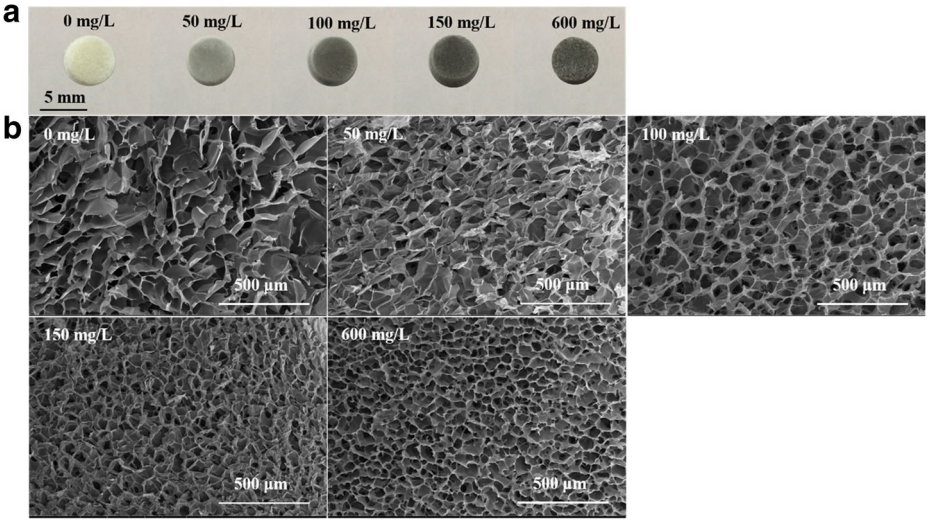

Fig. 1 Macro- and microscopic structural properties of GO/CS scaffolds. **a** Macrograph and **b** SEM micrographs of GO/CS scaffolds with different concentrations revealed that higher GO concentration yielded darker samples and smaller pore size samples

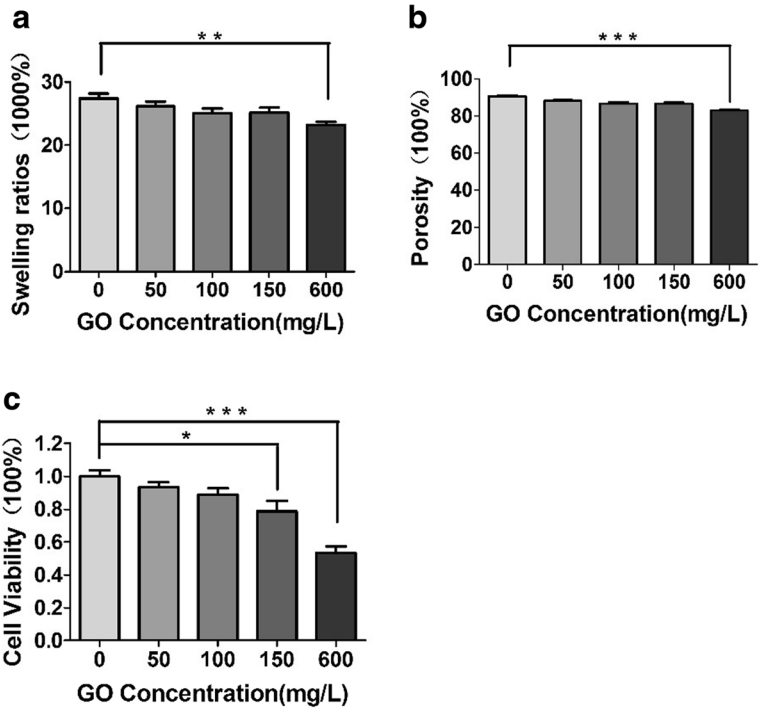

Fig. 2 Influence of GO concentration on swelling properties, porosity, and viability. **a** The swelling ratio and **b** the porosity of scaffolds decreased with GO concentration, but there were no significant differences compared with a non-GO scaffold (0 mg/L) unless 600 mg/L GO/CS scaffold ($p < 0.05$). **c** However, 600 mg/L GO/CS scaffold cause a significant reduction in cell viability (< 60%) ($p < 0.05$)

account the balance between physical characterization and cell survival rate. Therefore, 150 mg/L GO/CS scaffold was chosen to be used in the subsequent experiments.

Effect of GO on Electrical Conductivity

The electrical conductivity of GO/CS scaffolds was measured after the scaffolds were hydrated. A comparative analysis of the conductivity of the non-GO scaffold and 150 mg/L GO/CS scaffold were shown in Fig. 3. The slopes of the *I-V* curve represented the conductivity of the scaffolds. The 150 mg/L GO/CS scaffold (0.134 S/m) increased its conductivity compared with a non-GO scaffold (1.63×10^{-3} S/m). The results showed that GO could improve the electrical conductivity of the scaffolds.

Cardiomyocyte Morphology in the Scaffolds

To evaluate the effect of GO on cardiomyocyte morphology in scaffolds, SEM was taken to visualize cellular adhesion and extension of cells in scaffolds after 7 days of cultivation. Cells in non-GO (Fig. 4a, b) and GO/CS scaffolds (Fig. 4c–f) had secretion of extracellular matrix and exhibited a spherical morphology. Contrastively, it attached much more cells in GO/CS scaffolds (Fig. 4 D, F) than that in non-GO scaffolds (Fig. 4b). Moreover, abundant

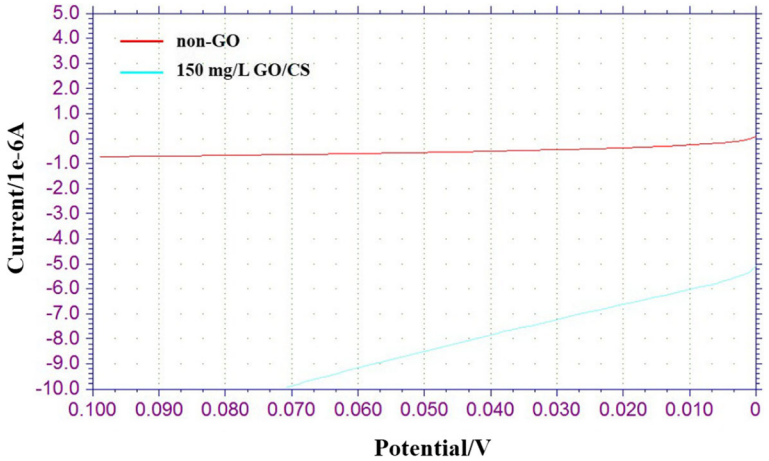

Fig. 3 Effect of GO on electrical conductivity. The GO/CS scaffold (0.134 S/m) markedly increased its conductivity compared with a non-GO scaffold (1.63×10^{-3} S/m). The results showed that GO could improve the electrical conductivity of the scaffolds

outstretched filopodia (as indicated by white arrows) were observed on cells in GO/CS scaffolds (Fig. 4d, f), which indicated the better cell–cell interactions.

Protein and Gene Expression of Cardiomyocytes in Scaffolds

To evaluate the effect of GO on the expression of specific cardiac proteins and genes, cardiac protein and gene expressions were analyzed for cardiomyocytes cultured in non-GO and GO/CS scaffolds. After 7 days of cultivation, it was observed that the expression of specific cardiac proteins in GO/CS scaffolds was stronger than that in the non-GO scaffold. There were significant increases in the expression of CX-43 (4.1-fold) and cTnT (1.3-fold) (Fig. 5a, b) ($p < 0.05$).

After 7 days of cultivation, significant upregulation of CX-43 gene (important for conduction of electrical signals) and downregulation of cTnT gene (important for contractile function) were observed in cells in GO/CS scaffolds (Fig. 5c) ($p < 0.05$). The expressions of two genes in cells in GO/CS scaffolds were different. The expression of CX-43 increased 2.3 folds, but the cTnT gene was downregulated to 0.88 fold. The higher CX43 protein and gene level on the seventh day, without electrical stimulation, suggested that GO affected physiology independently of possible complementary effects of the external electrical field.

Discussion

Development of conductive scaffold is of great importance in myocardial tissue engineering. In a recent study [28], they found that electrical stimulation induced remarkable enhancement of cell alignment, coupling, and ultrastructural organization. More and more researchers have confirmed that cardiac tissue engineering and electrical signal conduction are inseparable. In addition, scaffolds, made of either metal or metalloids such as carbon nanotube [29, 30], polypyrrole [15], graphene oxide flakes [19], and gold

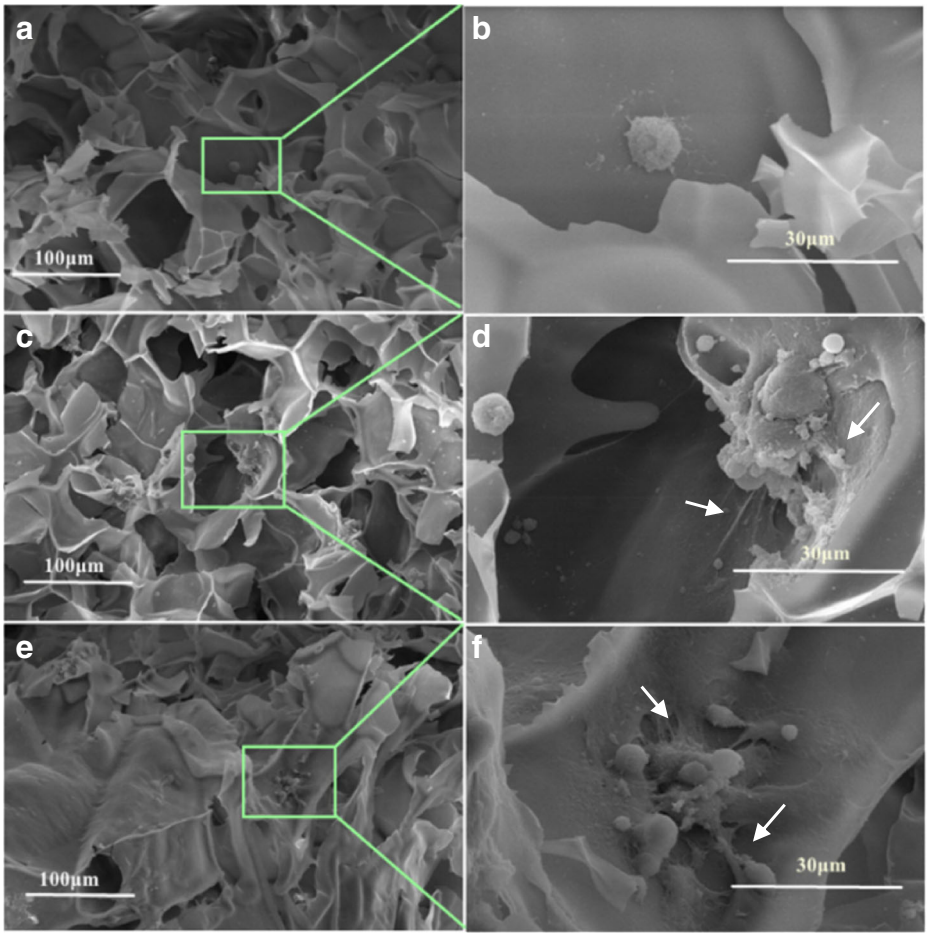

Fig. 4 Effect of GO on cardiomyocyte morphology in scaffolds. Cells in non-GO (**a**, **b**) and GO/CS scaffolds (**c**, **d**, **e**, **f**) had secretion of extracellular matrix and exhibited a spherical morphology. Contrastively, it was attached much more cells in GO/CS scaffolds (**d**, **f**) than that in non-GO scaffolds (**b**). Moreover, abundant outstretched filopodia (as indicated by white arrows) were observed on cells in GO/CS scaffolds (**d**, **f**), which indicated the better cell–cell interactions

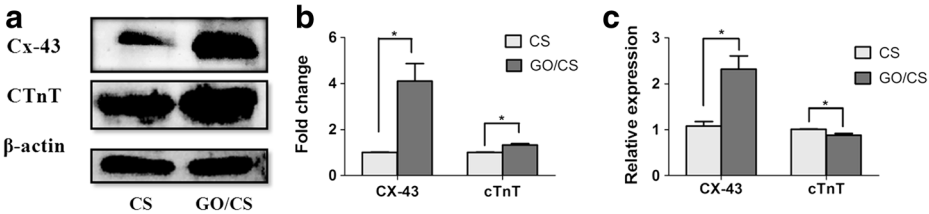

Fig. 5 Effect of GO on the expression of specific cardiac proteins and genes for cardiomyocytes cultured in scaffolds. After 7 days of culture, significant increases were observed in the expression of specific cardiac proteins in cells in GO/CS scaffolds, the expression of CX-43 and cTnT increased 4.1 and 1.3 folds, respectively (**a**, **b**) ($p < 0.05$). However, the expressions of two genes in cells in GO/CS scaffolds were different. The expression of CX-43 significantly increased 2.3 fold, but the cTnT gene was downregulated to 0.88 fold (**c**) ($p < 0.05$)

nanoparticle [7], have been used in cardiac tissue engineering because of their excellent electrical conductivity. In this study, using freezing and lyophilization, we described electrically conductive composite scaffolds based on CS, designed to have electrical conductivity properties similar to those of cardiac muscle by addition of GO.

Honeycomb scaffolds could overcome principal structural–mechanical limitations of scaffolds for myocardial tissue engineering [5]. Our data showed that scaffolds structure of GO/CS and non-GO, whether seeded with H9C2 rat myocardial cells or not, were homogeneous and not collapsed after 7 days of cultivation. It indicated that our three-dimensional porous scaffolds were strong and tough [23]. Furthermore, good scaffold's characteristics will benefit cell in-growth, vascularization, nutrient delivery, and metabolite transport [31]. In this study, we observed that the hydrophilicity and biocompatibility of GO/CS scaffolds did not weaken significantly due to the addition of GO.

Additionally, the formation of the extracellular matrix is very important for electrical signal conduction [32]. Our results found that large amounts of extracellular matrix were secreted by cardiac cells in GO/CS scaffolds. It demonstrated that GO/CS scaffold was excellent and could be applied in cardiac tissue engineering. GO has been verified that it could effectively prevent a series of adverse cell-signaling cascades for cardiac repair [19]. On the basis of these findings, we measured the conductivity of GO/CS and non-GO scaffolds, and found that GO could increase the conductivity of GO/CS scaffold. Moreover, we demonstrated that GO not only increased the conductivity of GO/CS scaffold but also enhanced the expressions of specific protein and gene (CX-43), involved in muscle contraction and electrical coupling, an observation broadly consistent with the previous works [33, 34]. Significant increase was observed in the expression of the cTnT protein in cells in GO/CS scaffolds, but the cTnT gene expression was significantly downregulated, which was consistent with the results of Gao et al. [35] and Hao et al [36] Our data confirmed that the presence of GO in CS scaffolds enhanced the cardiogenic phenotype and expression of cardiac markers after 7 days of cultivation, without external electrical stimulation. GO/CS scaffold is a suitable biomaterial for the application of cardiac tissue engineering.

Until now, the mechanism of GO/CS conductive scaffold increasing the capacity of cardiac tissue regeneration remains unclear. Several researchers have suggested that the conductivity of scaffold have the ability to induce cell alignment, elongation functional maturation, and anisotropy of myocardial cell between different layers [30]. A previous study demonstrated that GO flakes affected cardiac repair by enhancing secretion of reparative paracrine factors and reduced apoptosis of cardiac tissue [19]. Additionally, it was found that GO promoted the proliferation and spreading of the nerve cell [17]. In another study, graphene and GO accelerated the mesenchymal stem cell adhesion, proliferation, and differentiation [37]. In these studies, CX-43 was demonstrated to be the most important myogenic signal transmitted by cardiomyocyte. Here, we hypothesized that GO might promote the conductivity of the scaffolds to establish good signal conduction between the cells and the scaffolds. Then, the extracellular matrix increased with the increase of cell electrical physiological activity and CX-43 secretion. The extracellular matrix continued to participate in the transmission of electrical signals between cells and cells, and cells and scaffolds, to promote the electrical conductivity of cardiac myocytes and form a benign cycle. However, to get a more clear vision of regeneration cardiac tissue and eventual functionality of the construct, further investigations should be performed. Our future studies will focus on the application of GO/CS conductive scaffolds in vivo, particularly in myocardial infarction models.

Conclusion

In this study, we described electrically conductive composite scaffolds based on chitosan (CS), designed to have electrical conductivity properties similar to those of cardiac muscle by addition of graphene oxide (GO). The GO/CS scaffolds, supported adhesion and extension of cardiac cells, were better for cardiac cells clustered together and cell–cell interactions, and enhanced expression of specific cardiac proteins and genes without exogenous electrical stimulation.

Funding This study was supported by the National Key Research and Development Program of China (2017YFC1702006), the National Natural Science Foundation of China [31400307], the Fundamental Research Funds for the Central Universities [DUT14RC(3)016, DUT16RC(4)73]; the Liaoning Natural Science Foundation of China [201601033]; and the General Projects of Liaoning Education Department Science and Research Foundation [L2015111].

Compliance with Ethical Standards

Conflict of Interest The authors declare that they have no competing interests.

Publisher's Note Springer Nature remains neutral with regard to jurisdictional claims in published maps and institutional affiliations.

References

1. Kikuchi, K., & Poss, K. D. (2012). Cardiac regenerative capacity and mechanisms [J]. *Annual Review of Cell and Developmental Biology, 28*(1), 719–741.
2. Dvir, T., Timko, B. P., Brigham, M. D., Naik, S. R., Karajanagi, S. S., Levy, O., Jin, H., Parker, K. K., Langer, R., & Kohane, D. S. (2011). Nanowired three-dimensional cardiac patches [J]. *Nature Nanotechnology, 6*(11), 720–725.
3. Wang, F., & Guan, J. (2010). Cellular cardiomyoplasty and cardiac tissue engineering for myocardial therapy [J]. *Advanced Drug Delivery Reviews, 62*(7–8), 784–797.
4. Dai, X., Zhou, W., Gao, T., Liu, J., & Lieber, C. M. (2016). Three-dimensional mapping and regulation of action potential propagation in nanoelectronics-innervated tissues [J]. *Nature Nanotechnology, 11*(9), 776–782.
5. Engelmayr, G. C., Jr., Cheng, M., Bettinger, C. J., Borenstein, J. T., Langer, R., & Freed, L. E. (2008). Accordion-like honeycombs for tissue engineering of cardiac anisotropy [J]. *Nature Materials, 7*(12), 1003–1010.
6. Shin, S. R., Aghaei-Ghareh-Bolagh, B., Gao, X., Nikkhah, M., Jung, S. M., Dolatshahi-Pirouz, A., Kim, S. B., Kim, S. M., Dokmeci, M. R., Tang, X. S., & Khademhosseini, A. (2014). Layer-by-layer assembly of 3D tissue constructs with functionalized graphene [J]. *Advanced Functional Materials, 24*(39), 6136–6144.
7. Baei, P., Jalili-Firoozinezhad, S., Rajabi-Zeleti, S., Tafazzoli-Shadpour, M., Baharvand, H., & Aghdami, N. (2016). Electrically conductive gold nanoparticle-chitosan thermosensitive hydrogels for cardiac tissue engineering [J]. *Materials Science & Engineering, C: Materials for Biological Applications, 63*, 131–141.
8. Martins, A. M., Eng, G., Caridade, S. G., Mano, J. F., Reis, R. L., & Vunjak-Novakovic, G. (2014). Electrically conductive chitosan/carbon scaffolds for cardiac tissue engineering [J]. *Biomacromolecules, 15*(2), 635–643.
9. Jithendra, P., Rajam, A. M., Kalaivani, T., Mandal, A. B., & Rose, C. (2013). Preparation and characterization of aloe vera blended collagen-chitosan composite scaffold for tissue engineering applications [J]. *ACS Applied Materials & Interfaces, 5*(15), 7291–7298.
10. Choi, B., Kim, S., Lin, B., Wu, B. M., & Lee, M. (2014). Cartilaginous extracellular matrix-modified chitosan hydrogels for cartilage tissue engineering [J]. *ACS Applied Materials & Interfaces, 6*(22), 20110–20121.
11. Philibert, T., Lee, B. H., & Fabien, N. (2017). Current status and new perspectives on chitin and chitosan as functional biopolymers [J]. *Applied Biochemistry and Biotechnology, 181*(4), 1314–1337.
12. Zhang, T., Jin, L., Fang, Y., Lin, F., Sun, W., & Xiong, Z. (2014). Fabrication of biomimetic scaffolds with oriented porous morphology for cardiac tissue engineering [J]. *Journal of Biomaterials and Tissue Engineering, 4*(12), 1030–1039.

13. Rabbani, S., Soleimani, M., Imani, M., Sahebjam, M., Ghiaseddin, A., Nassiri, S. M., Majd Ardakani, J., Tajik Rostami, M., Jalali, A., Mousanassab, B., Kheradmandi, M., & Ahmadi Tafti, S. H. (2017). Regenerating heart using a novel compound and human Wharton jelly mesenchymal stem cells [J]. *Archives of Medical Research, 48*(3), 228–237.
14. Zhu, Y. X., Song, K. D., Jiang, S. Y., Chen, J. L., Tang, L. Z., Li, S. Y., Fan, J., Wang, Y., Zhao, J., & Liu, T. (2017). Numerical simulation of mass transfer and three-dimensional fabrication of tissue-engineered cartilages based on chitosan/gelatin hybrid hydrogel scaffold in a rotating bioreactor [J]. *Applied Biochemistry and Biotechnology, 181*(1), 250–266.
15. Mihic, A., Cui, Z., Wu, J., Vlacic, G., Miyagi, Y., Li, S. H., Lu, S., Sung, H. W., Weisel, R. D., & Li, R. K. (2015). A conductive polymer hydrogel supports cell electrical signaling and improves cardiac function after implantation into myocardial infarct [J]. *Circulation, 132*(8), 772–784.
16. Seokwon, P., Flavia, V., Eichmann, S. L., Benavides, O. M., Matteo, P., & Jacot, J. G. (2014). Biocompatible carbon nanotube-chitosan scaffold matching the electrical conductivity of the heart [J]. *ACS Nano, 28*(8), 10.
17. Liu, X., Miller, A. L., 2nd, Park, S., Waletzki, B. E., Zhou, Z., Terzic, A., et al. (2017). Functionalized carbon nanotube and graphene oxide embedded electrically conductive hydrogel synergistically stimulates nerve cell differentiation [J]. *ACS Applied Materials & Interfaces, 9*(17), 14677–14690.
18. Jing, X., Mi, H.-Y., Napiwocki, B. N., Peng, X.-F., & Turng, L.-S. (2017). Mussel-inspired electroactive chitosan/graphene oxide composite hydrogel with rapid self-healing and recovery behavior for tissue engineering [J]. *Carbon, 125*, 557–570.
19. Jooyeon, P., Bokyoung, K., Jin, H., Jaewon, O., Subeom, P., Seungmi, R., et al. (2015). Graphene oxide flakes as a cellular adhesive: prevention of reactive oxygen species mediated death of implanted cells for cardiac repair [J]. *ACS Nano, 26*(9), 5.
20. Waiwijit, U., Maturos, T., Pakapongpan, S., Phokharatkul, D., Wisitsoraat, A., & Tuantranont, A. (2016). Highly cytocompatible and flexible three-dimensional graphene/polydimethylsiloxane composite for culture and electrochemical detection of L929 fibroblast cells [J]. *Journal of Biomaterials Applications, 31*(2), 230–240.
21. Han, Y., Zeng, Q., Li, H., & Chang, J. (2013). The calcium silicate/alginate composite: preparation and evaluation of its behavior as bioactive injectable hydrogels [J]. *Acta Biomaterialia, 9*(11), 9107–9117.
22. Shamekhi, M. A., Rabiee, A., Mirzadeh, H., Mahdavi, H., Mohebbi-Kalhori, D., & Baghaban, E. M. (2017). Fabrication and characterization of hydrothermal cross-linked chitosan porous scaffolds for cartilage tissue engineering applications [J]. *Materials Science & Engineering, C: Materials for Biological Applications, 80*, 532–542.
23. Wan, S., Peng, J., Li, Y., Hu, H., Jiang, L., & Cheng, Q. (2015). Use of synergistic interactions to fabricate strong, tough, and conductive artificial nacre based on graphene oxide and chitosan [J]. *ACS Nano, 9*(10), 9830–9836.
24. Thein-Han, W. W., & Misra, R. D. (2009). Biomimetic chitosan-nanohydroxyapatite composite scaffolds for bone tissue engineering [J]. *Acta Biomaterialia, 5*(4), 1182–1197.
25. Stout, D. A., Yoo, J., Santiago-Miranda, A. N., & Webster, T. J. (2012). Mechanisms of greater cardiomyocyte functions on conductive nanoengineered composites for cardiovascular application [J]. *International Journal of Nanomedicine, 7*, 5653–5669.
26. Roell, W., Lewalter, T., Sasse, P., Tallini, Y. N., Choi, B. R., Breitbach, M., Doran, R., Becher, U. M., Hwang, S. M., Bostani, T., von Maltzahn, J., Hofmann, A., Reining, S., Eiberger, B., Gabris, B., Pfeifer, A., Welz, A., Willecke, K., Salama, G., Schrickel, J. W., Kotlikoff, M. I., & Fleischmann, B. K. (2007). Engraftment of connexin 43-expressing cells prevents post-infarct arrhythmia [J]. *Nature, 450*(7171), 819–824.
27. Kim, Y. H., Choi, S. H., D'Avanzo, C., Hebisch, M., Sliwinski, C., Bylykbashi, E., Washicosky, K. J., Klee, J. B., Brüstle, O., Tanzi, R. E., & Kim, D. Y. (2015). A 3D human neural cell culture system for modeling Alzheimer's disease [J]. *Nature Protocols, 10*(7), 985–1006.
28. Radisic, M., Park, H., Shing, H., Consi, T., Schoen, F. J., Langer, R., Freed, L. E., & Vunjak-Novakovic, G. (2004). Functional assembly of engineered myocardium by electrical stimulation of cardiac myocytes cultured on scaffolds [J]. *Proceedings of the National Academy of Sciences of the United States of America, 101*(52), 18129–18134.
29. Pok, S., Vitale, F., Eichmann, S. L., Benavides, O. M., Pasquali, M., & Jacot, J. G. (2015). Biocompatible carbon nanotube-chitosan scaffold matching the electrical conductivity of the heart [J]. *ACS Nano, 8*(10), 9822–9832.
30. Wu, Y., Wang, L., Guo, B., & Ma, P. X. (2017). Interwoven aligned conductive nanofiber yarn/hydrogel composite scaffolds for engineered 3D cardiac anisotropy [J]. *ACS Nano, 11*(6), 5646–5659.
31. Hollister, S. (2005). Porous scaffold design for tissue engineering [J]. *Nature Materials, 4*(7), 518–524.
32. Jang, J., Park, H. J., Kim, S. W., Kim, H., Park, J. Y., Na, S. J., Kim, H. J., Park, M. N., Choi, S. H., Park, S. H., Kim, S. W., Kwon, S. M., Kim, P. J., & Cho, D. W. (2017). 3D printed complex tissue construct using stem cell-laden decellularized extracellular matrix bioinks for cardiac repair [J]. *Biomaterials, 112*, 264–274.

33. You, J. O., Rafat, M., Ye, G. J., & Auguste, D. T. (2011). Nanoengineering the heart: conductive scaffolds enhance connexin 43 expression [J]. *Nano Letters, 11*(9), 3643–3648.
34. Shin, S. R., Jung, S. M., Zalabany, M., Kim, K., Zorlutuna, P., Kim, S. B., et al. (2013). Carbon-nanotube-embedded hydrogel sheets for engineering cardiac constructs and bioactuators [J]. *ACS Nano, 7*(3), 2369–2380.
35. Gao, Y., Connell, J. P., Wadhwa, L., Ruano, R., & Jacot, J. G. (2014). Amniotic fluid-derived stem cells demonstrated cardiogenic potential in indirect co-culture with human cardiac cells [J]. *Annals of Biomedical Engineering, 42*(12), 2490–2500.
36. Hao, T., Zhou, J., Lu, S., Yang, B., Wang, Y., Fang, W., et al. (2016). Fullerene mediates proliferation and cardiomyogenic differentiation of adipose-derived stem cells via modulation of MAPK pathway and cardiac protein expression [J]. *International Journal of Nanomedicine, 11*, 269–283.
37. Wong Cheng, L., Lim, C. H. Y. X., Hui, S., Tang, L. A. L., Yu, W., Chwee Teck, L., et al. (2011). Origin of enhanced stem cell growth and differentiation on graphene and graphene oxide [J]. *ACS Nano, 27*(5), 9.